Nonlinear analysis of traffic jams in an anisotropic continuum model

2010 Chinese Phys. B 19 110503

(http://iopscience.iop.org/1674-1056/19/11/110503)

Chin. Phys. B Vol. 19, No. 11 (2010) 110503

Nonlinear analysis of traffic jams in an anisotropic continuum model

Arvind Kumar Gupta[a)†] and Sapna Sharma[b)]

[a)] *Department of Mathematics, IIT Ropar-140001, India*
[b)] *Mathematics Group, Birla Institute of Technology and Science, Pilani-333031, India*

(Received 4 November 2009; revised manuscript received 18 May 2010)

This paper presents our study of the nonlinear stability of a new anisotropic continuum traffic flow model in which the dimensionless parameter or anisotropic factor controls the non-isotropic character and diffusive influence. In order to establish traffic flow stability criterion or to know the critical parameters that lead, on one hand, to a stable response to perturbations or disturbances or, on the other hand, to an unstable response and therefore to a possible congestion, a nonlinear stability criterion is derived by using a wavefront expansion technique. The stability criterion is illustrated by numerical results using the finite difference method for two different values of anisotropic parameter. It is also been observed that the newly derived stability results are consistent with previously reported results obtained using approximate linearisation methods. Moreover, the stability criterion derived in this paper can provide more refined information from the perspective of the capability to reproduce nonlinear traffic flow behaviors observed in real traffic than previously established methodologies.

Keywords: traffic flow, non-linear stability, wavefront method
PACC: 0520

1. Introduction

Since an efficient traffic system is very important to modern industrialised countries, the investigation of traffic flow problems is a very attentive topic of deliberation and researched for scientists and engineers nowadays. In the early stage of traffic engineering development, the methods to solve the traffic problems and design roads were largely empirical, built upon observations, measurements and statistical analyses. Apart from the experimental observations, many physical models have been proposed.[1,2] An important question regarding the applicabilities of these models lies in their capability to validate the empirical data collected by traffic flow studies to compare their models predictions with the real world situations. Each of these models has been tested either by simulation or against actual traffic flow measurements. Unfortunately, such validation processes have always invalidated the models.[3] Traditionally, these models are classified into two types: microscopic ones and macroscopic ones. The former simulates the motion of every vehicle while the latter concentrates on the collective behaviour of vehicles. Macroscopic models give an overview of the global traffic flow, which is needed for understanding the collective behaviour of traffic and more suitable for real-time simulations, short-term traffic predictions, developing and controlling on-line speed-control systems and evaluating average travel time, fuel consumption and vehicle emissions etc.

The development of the macroscopic traffic flow models began with the LWR model developed independently by Lighthill and Whitham,[4] and Richards[5] for a homogeneous and unidirectional highway. The LWR model is known as the simple continuum model in which the relationships among the three aggregate variables (q, v and ρ) are modeled. The LWR model employs the conservation equation in the following form:

$$\rho_t + q_x = 0, \tag{1}$$

and is supplemented by the following equation of traffic flow:

$$q = \rho v, \tag{2}$$

and a relationship between the mean speed and the traffic density under equilibrium conditions

$$v = V_{\mathrm{e}}(\rho), \tag{3}$$

where $V_{\mathrm{e}}(\rho)$ is the generalised equilibrium velocity, which is given by the steady state relationship between highway velocity and density (e.g. fundamental

†Corresponding author. E-mail: arvigupta@gmail.com

diagrams). Here x and t represent space and time respectively.

The above LWR model, the simplest among all the continuum models exhibits a wide range of phenomena such as traffic 'sound' waves, shocks and rarefaction waves. The consistency and the existence of weak solution of such conservation laws have been studied by Zhang[6] and Lax,[7] respectively.

However, the LWR model has its deficiencies, the most fatal one is that the speed is solely determined by the equilibrium speed density relationship. No fluctuation of speed around the equilibrium values is allowed, thus, the model is not suitable for the description of non-equilibrium situations like stop-and-go traffic etc.

In the past decades, many efforts were devoted to improve the LWR model through developing higher-order models, which use dynamic equation for the speed to replace the equilibrium relationship (3). Perhaps the most well known result of these efforts is the higher order model developed by Payne.[8] In the Payne model, the fluctuation of speed around the equilibrium values is allowed, thus, the model is suitable for the description of non-equilibrium situations like stop-and-go traffic etc. The dynamic equation of Payne's model is derived from car-following theory and has the following form:

$$v_t + vv_x = \frac{V_{\rm e}(\rho) - v}{\tau} + \frac{V'_{\rm e}(\rho)}{2\tau\rho}\rho_x, \tag{4}$$

where τ is the relaxation time and $V'_{\rm e}(\rho) = \partial V_{\rm e}(\rho)/\partial\rho$.

Later several authors[9−11] have suggested a considerable number of modifications to Payne's model.[8] Berg *et al.*[12] proposed a continuum version of the car following optimal velocity model[13] by using a series expansion of the headway in terms of the density.

However, as pointed out by Daganzo,[14] it was shown that the Payne model (and the other listed nonequilibrium models) had two families of characteristic, along which traffic information is transmitted: one is slower and the other is faster than the speed of the traffic stream that carries them. The faster characteristic leads to a gas-like behaviour which means that the vehicle from behind can force the vehicles in front to speed up,[15] and diffusion causes 'wrong way' travel.[14] One fundamental principal of the traffic flow is that vehicles are anisotropic and respond only to the frontal stimuli. Treiber *et al.*[16] in his gas kinetic traffic model (GKT) has solved the issue of wrong way travel problems. Zhang[17,18] has proposed new non-equilibrium models and shown that the new models overcome the backward travel problem. Recently, Gupta and Katiyar[19,20] developed an improved anisotropic continuum model based upon the car following model given by Jiang *et al.*[21] and using the series expansion between headway and density given by Berg *et al.*[12]

The applicability of all the existing traffic flow models depends on their capability to replicate how traffic congestions occur when disturbances are present in transportation systems. There is a large body of research that deals with the stability of traffic flow. Holland[22] discussed traffic stability for various well-known microscopic traffic flow models i.e. car following models. Witham[23] presented a stability criterion for a well-known second order macroscopic traffic flow model known as the Payne–Whitham (PW) model. Swaroop and Rajagopal[24] introduce a formal definition of traffic flow stability based on the macroscopic traffic flow description and related it to string stability based on a car-following model. The stability of a new higher order continuum model introduced by Zhang[25] and the PW model is analysed by Zhang.[25] Del Castillo[26] discussed the propagation of perturbations in traffic flow using a stochastic approximation approach in a microscopic model.

Since perturbations propagate in the form of waves, most wave methods can be used to study them. For example, studies on small perturbations on a traffic flow model can be done by the linearised method. However, large perturbations are still less discussed in related literature. A nonlinear technique to analyse the shock wave propagation properties of a class of second order continuum traffic flow models of Payne type is given by Yi *et al.*[27] A nonlinear stability criterion is derived using a wavefront expansion technique. Ou *et al.*[28] discussed the nonlinear analysis in the ARA model of traffic flow. The equilibrium functions of traffic flow are investigated in the light of stability using wavefront technique by Ou *et al.*[29,30] Recently, Helbing and Johansson[31] revisit the argument of Daganzo[14] by linking the characteristic speeds with the group velocities of the wave packets arising from sinusoidal excitations to the linearised equations. They presented new arguments against the notion that faster-than-traffic characteristic speeds constitute a theoretical inconsistency of traffic flow models. Zhang[32] showed that faster-than-traffic characteristics produce counterintuitive predic-

tions and a linear stability analysis is not able to explain it.

In this work, we analyse the effect of large perturbation using the wavefront expansion technique in a recently developed continuum model.[19,20] This new model overcomes the problem of negative flows and negative speeds (i.e., wrong-way travel) that exists in almost every higher-order continuum models and therefore can describe the traffic-flow dynamics more realistically.

In the next section, we present an improved continuum model recently developed by the author.[19,20] In Section 3, we analyse some qualitative features of the model and in Section 4, we study its stability properties. We then discussed the numerical technique in Section 5 and finally in Section 6, we provide a discussion on our results.

2. A New anisotropic continuum model

In this work, we adopt the one-lane continuum traffic-flow model, which was first introduced in Refs. [19] and [20] The model contains a continuity equation which relates the local density $\rho(x,t)$ of the traffic to the average speed $v(x,t)$

$$\rho_t + (\rho v)_x = 0. \tag{5}$$

The average traffic speed v obeys an evolution equation similar to the Navier–Stokes equation, but with some distinctive characteristics

$$v_t + v v_x = a\left[V_{\mathrm{e}}(\rho) - v\right] + \frac{a V_{\mathrm{e}}'(\rho)\,\rho_x}{2\rho} - 2\beta\, c(\rho)\, v_x, \tag{6}$$

where $c^2(\rho) = -a\,V_{\mathrm{e}}'(\rho)/2$.

The first term on the right side of Eq. (6) called the relaxation term, describes the adaptation of the average speed $v(x,t)$ to the density dependent equilibrium speed $V_{\mathrm{e}}(\rho)$. This adaptation is exponential in time with the driver's reaction time ($\tau = 1/a$). The second term, called the anticipation term, reflects the reaction of identical drivers to the traffic situation in their surroundings. As pointed out by Zhang,[11] we neglected the higher order terms as they do not have any significant effect on qualitative properties of the proposed model.[19,20] It can be seen in the next section.

3. Traffic flow characteristics

In this section, we will discuss the qualitative properties of the given system. All perturbations propagate along characteristic curves on the highway. Therefore, the characteristics of a traffic system give intrinsic information regarding wave propagation.[27] To analyse the traffic flow stability, we need to first investigate the characteristic velocity of the traffic flow system given by Eqs. (5) and (6).

The full differentials of $\rho(x,t)$ and $v(x,t)$ are given by

$$\mathrm{d}\rho(x,t) = \rho_x \mathrm{d}x + \rho_t \mathrm{d}t, \tag{7}$$

$$\mathrm{d}y(x,t) = v_x \mathrm{d}x + v_t \mathrm{d}t. \tag{8}$$

We rewrite the Eqs. (5)–(8) in matrix notation as follows:

$$\begin{bmatrix} 1 & v & 0 & \rho \\ 0 & -\dfrac{aV_{\mathrm{e}}'(\rho)}{2\rho} & 1 & v + 2\beta c(\rho) \\ \mathrm{d}t & \mathrm{d}x & 0 & 0 \\ 0 & 0 & \mathrm{d}t & \mathrm{d}x \end{bmatrix} \begin{bmatrix} \rho_t \\ \rho_x \\ v_t \\ v_x \end{bmatrix} = \begin{bmatrix} 0 \\ \dfrac{V_{\mathrm{e}} - v}{\tau} \\ \mathrm{d}\rho \\ \mathrm{d}v \end{bmatrix}. \tag{9}$$

In order to get the discontinuous solution for $\rho(x,t)$ and $v(x,t)$, the coefficient matrix of partial derivatives should be singular. Thus the characteristic velocities are given by

$$v_{c_1} = \left(\frac{\mathrm{d}x}{\mathrm{d}t}\right)_1 = v + \left(\beta + \sqrt{1+\beta^2}\right)\, c(\rho), \tag{10}$$

$$v_{c_2} = \left(\frac{\mathrm{d}x}{\mathrm{d}t}\right)_2 = v + \left(\beta - \sqrt{1+\beta^2}\right)\, c(\rho). \tag{11}$$

For first characteristic field the properties of these waves are quantitatively identical to those of the LWR model because of $(\mathrm{d}x/\mathrm{d}t)_1 \leq v$. But for the second characteristic, the waves behaves quite differently as they travel faster than traffic ($(\mathrm{d}x/\mathrm{d}t)_2 \geq v$). This means that the future conditions of the traffic flow will be affected by the traffic conditions behind the flow. Such type of behaviour, however, can be controlled by the factor β in our model. We call it the anisotropic factor. Note that for $\beta \gg 1$, the second characteristic approaches v, the velocity of the traffic. Thus, information can never reach vehicles from behind. The term having this anisotropic factor in the system (6) is known as an anisotropic term.

4. Global stability analysis

When the traffic jam happens, the density of the traffic jam is much higher than that of the neighbouring section, so most traffic jams belong to large disturbances. When the disturbance is fairly large, the linearisation method may produce incorrect results because of neglecting higher-order terms as pointed out by Whitham,[23] which is the primary cause we propose a nonlinear stability analysis for traffic flow.[23,27−30]

In order to check whether the new developed anisotropic model can describe the nonlinear theory of the cluster effect under large perturbation in a traffic flow, i.e., the effect of the appearance of a region of high density and low average velocity of vehicles in an initially homogeneous flow, in this section we study the propagation stability conditions using wavefront expansion methods. If a disturbance starts at position x_0 in the homogeneous state of traffic flow, the wavefront is the propagation curve of the disturbance along the homogeneous traffic flow.[23,27−30] The magnitude of the initial disturbance will not increase during its propagation if the traffic system is stable in propagation; otherwise, a disturbed density or velocity wave may increase in magnitude as it propagates upstream and ultimately form a shock wave or traffic jam on the highway. If the form of the initial density disturbance is given, the initial velocity disturbance can be determined by the equilibrium function. Furthermore, the profiles of density and velocity disturbances are symmetrical to some degree along the x-axis in the simulation with the continuum model (e.g., monotone increase vs. monotone decrease, concavity vs. convexity, etc.),[10,33,34] which is still considered valid in our model. Therefore, when we merely demand some mathematical assumptions for the density, they are automatically needed for the velocity, and most results are presented for either the density or the velocity.

Through nonlinear stability analysis on the macroscopic traffic flow model, a stability criterion and stability-judging parameters for macroscopic stability can be obtained. Assume that a disturbance initiates from the equilibrium state $(\rho_0, v_0 = V_\mathrm{e}(\rho_0))$, the solutions of Eqs. (5) and (6), in the homogeneous traffic flow. If the mth derivatives of ρ around the wavefront are the first ones to be discontinuous, the expanded Taylor series from ρ_0 starts with the term in the mth power of a small parameter, which is equally assumed for v_0.

The analogous criterion for the continuum model may be found by expanding the solution of the system around the wavefront in powers of

$$\xi = x - X(t), \tag{12}$$

where $X(t)$ is the location of the wavefront at time t. Since the wavefront is the boundary of the disturbance in the homogeneous state, the characteristic method is still feasible in some small neighbourhood of the wavefront. Therefore the wavefront has the characteristic velocity $v_{c_{1,2}}$ in the equilibrium states, i.e.

$$\dot{X}(t) = v_{c_{1,2}}(\rho_0, v_0) = v + \left(\beta \pm \sqrt{1+\beta^2}\right) c(\rho). \tag{13}$$

Without loss of generality, we can assume that the first derivative of the density profile around the wavefront is discontinuous. Using Eq. (12), we can expand the flow variables ρ and v behind the wavefront in a power series of ξ as

$$\rho(x,t) = \rho_0 + \xi\rho_1(t) + \frac{1}{2}\xi^2\rho_2(t) + \ldots, \tag{14}$$

$$v(x,t) = v_0 + \xi v_1(t) + \frac{1}{2}\xi^2 v_2(t) + \ldots, \tag{15}$$

where

$$\rho_i(t) = \left.\frac{\partial^i \rho}{\partial x^i}\right|_{(X(t)^-,t)},$$

$$v_i(t) = \left.\frac{\partial^i v}{\partial x^i}\right|_{(X(t)^-,t)}, \quad i = 1,2,3,\ldots.$$

Using Eqs. (14) and (15), the partial derivatives of the state variables ρ and v can be calculated as

$$\rho_t = -\dot{X}(t)\rho_1(t) + \xi\dot{\rho}_1(t) + \xi\left(-\dot{X}(t)\right)\rho_2(t) + \frac{1}{2}\xi^2\dot{\rho}_2(t) + \ldots, \tag{16}$$

$$\rho_x = \rho_1(t) + \xi\rho_2(t) + \frac{1}{2}\xi^2\rho_3(t) + \ldots, \tag{17}$$

$$v_t = -\dot{X}(t)\, v_1(t) + \xi \dot{v}_1(t) + \xi\left(-\dot{X}(t)\right) v_2(t) + \frac{1}{2}\xi^2 \dot{v}_2(t) + \ldots, \quad (18)$$

$$v_x = v_1(t) + \xi v_2(t) + \frac{1}{2}\xi^2 v_3(t) + \ldots. \quad (19)$$

Similarly for $V_{\mathrm{e}}(\rho)$ and $c(\rho)$, we obtain

$$V_{\mathrm{e}}(\rho, v) = V_{\mathrm{e}}^0 + \xi\left[V_{e,\rho}^0 \rho_1(t) + V_{e,v}^0 v_1(t)\right] + \ldots, \quad (20)$$

$$c(\rho, v) = c^0 + \xi\left[c_\rho^0 \rho_1(t) + c_v^0 v_1(t)\right] + \ldots, \quad (21)$$

where

$$V_{\mathrm{e}}^0 = V_{\mathrm{e}}(\rho_0), \quad V_{e,\rho}^0 = \left.\frac{\partial V_{\mathrm{e}}}{\partial \rho}\right|_{(\rho_0, v_0)},$$
$$V_{e,v}^0 = \left.\frac{\partial V_{\mathrm{e}}}{\partial v}\right|_{(\rho_0, v_0)}, \quad c^0 = c(\rho_0),$$
$$c_\rho^0 = \left.\frac{\partial c}{\partial \rho}\right|_{(\rho_0, v_0)}, \quad \text{and} \quad c_v^0 = \left.\frac{\partial c}{\partial v}\right|_{(\rho_0, v_0)}.$$

Substituting Eqs. (14)–(21) into the system (5) and (6), for the coefficients of the orders of magnitude ξ^0 and ξ^1, we obtain

$$-u_0\rho_1 + \rho_0 v_1 = 0, \quad (22)$$

$$\dot{\rho}_1 - \rho_2 u_0 + 2\rho_1 v_1 + \rho_0 v_2 = 0, \quad (23)$$

$$-u_0 v_1 \rho_0 - \frac{a}{2} V_{e,\rho}^0 \rho_1 + 2\beta c^0 v_1 \rho_0 = 0, \quad (24)$$

$$-\rho_0 u_0 v_2 + \dot{v}_1 \rho_0 - u_0 v_1 \rho_1 + \rho_0 v_1^2 - a\rho_0\left(V_{e,\rho}^0 \rho_1 + V_{e,v}^0 v_1 - v_1\right) - \frac{a}{2}\left(V_{e,\rho}^0 \rho_2 + \rho_1\left(V_{e,\rho\rho}^0 \rho_1 + V_{e,\rho v}^0 v_1\right)\right) + 2\beta\left(v_1\rho_0\left(c_\rho^0 \rho_1 + c_v^0 v_1\right) + v_1\rho_1 c^0 + v_2\rho_0 c^0\right) = 0, \quad (25)$$

where $u_0 = \left(\beta + \sqrt{1+\beta^2}\right) c(\rho)$ and for our model, $V_{\mathrm{e,v}}^0 = 0$, $V_{\mathrm{e},\rho\mathrm{v}}^0 = 0$, and $c_v^0 = 0$. For Eqs. (23) and (25), notice that the coefficient of ρ_2 and v_2 are linearly dependent since

$$\det\begin{vmatrix} -u_0 & \rho_0 \\ -\dfrac{aV_{e,\rho}^0}{2} & -u_0\rho_0 + 2\beta c^0 \rho_0 \end{vmatrix} = u_0^2\rho_0 - 2\beta c^0 u_0 \rho_0 + \frac{aV_{e,\rho}^0 \rho_0}{2} = 0, \quad (26)$$

and therefore, ρ_2 and v_2 can be eliminated. Putting $\rho_1 = \rho_0 v_1/u_0$ in Eqs. (23) and (25), we get the Bernoulli equation:

$$\dot{v}_1 + A v_1 + B v_1^2 = 0, \quad (27)$$

where

$$A = \frac{a\left(\rho_0 u_0 - \rho_0^2 V_{e,\rho}^0\right)}{2u_0 - 2\beta c^0 \rho_0},$$

$$B = 1 + \frac{4\beta\rho_0 u_0 c_\rho^0 - aV_{e,\rho\rho}^0 \rho_0}{4u_0\left(u_0 - \beta c^0\right)}.$$

The above Bernoulli equation gives the slope evolution at the wavefront and its propagation stability can be analysed in terms of the initial condition $v_1(0)$ and the parameters A and B.[27] The value of B is always greater than 1 for both the characteristic velocity.

If $A = 0$, the solution of Eq. (27) is

$$v_1(t) = \frac{v_1(0)}{\beta t v_1(0) + 1}, \quad (28)$$

whose monotonicity is determined by

$$\dot{v}_1(t) = -\frac{\beta v_1^2(0)}{\left(\beta t v_1(0) + 1\right)^2}. \quad (29)$$

If $A \neq 0$, the general solution of Eq. (27) is given as

$$v_1(t) = \frac{A}{B}\frac{\mathrm{e}^{-At}}{\left(1 + \dfrac{A}{Bv_1(0)}\right) - \mathrm{e}^{-At}}, \quad (30)$$

whose monotonicity is determined by

$$\dot{v}_1(t) = -\frac{A^2}{B}\frac{\left(1 + \dfrac{A}{Bv_1(0)}\right)\mathrm{e}^{-At}}{\left\{\left(1 + \dfrac{A}{Bv_1(0)}\right) - \mathrm{e}^{-At}\right\}^2}. \quad (31)$$

Therefore we can judge the trend of $v_1(t)$ in the light of the parameter A and the initial equilibrium state according to Table 1. Without loss of generality, if the density disturbance is upward, the velocity perturbation is downward, i.e., $v_1(0) < 0$. If $v_1(0) \in [-A/B, 0]$, the stability criterion for the system (5) and (6) is

$$A = \frac{a\left(\rho_0 u_0 - \rho_0^2 V_{e,\rho}^0\right)}{2u_0 - 2\beta c^0 \rho_0} > 0, \quad (32)$$

or

$$u_0 < \rho_0 V_{e,\rho}^0. \quad (33)$$

This shows that the model is stable against all large perturbations for the inequality (33). Consequently, the instability criterion is $A < 0$. In order to introduce metastability and its critical and marginal property into mathematical analysis, its stability criterion deduces $A \approx 0$.

Table 1. Stability conditions for the system given by Eq. (27).

parameter A	stable region	unstable region
$A > 0$	$v_1(0) \in (-A/B, +\infty)$, $v_1(t) \to 0$	$v_1(0) \in (-\infty, -A/B)$, $v_1(t) \to -\infty$
$A = 0$	$v_1(0) \in (0, +\infty)$, $v_1(t) \to 0$	$v_1(0) \in (-\infty, 0)$, $v_1(t) \to -\infty$
$A < 0$	$v_1(0) \in (0, +\infty)$, $v_1(t) \to -A/B$	$v_1(0) \in (-\infty, 0)$, $v_1(t) \to -\infty$

5. Numerical scheme and computational experiment

5.1. Solution procedure

In this section we present the numerical solution method. In doing so, the freeway to be modeled is divided into I nodes and the period of analysis into J time steps. The following difference equations are obtained by applying the finite difference method on the system of Eqs. (5) and (6)

$$\rho_i^{j+1} = \rho_i^j + \frac{\Delta t}{\Delta x}\rho_i^j(v_i^j - v_{i+1}^j) + \frac{\Delta t}{\Delta x}v_i^j(\rho_{i-1}^j - \rho_i^j); \tag{34}$$

a) For heavy traffic (i.e. $v_i^j < -2\beta\, c(\rho)$)

$$v_i^{j+1} = v_i^j + \frac{\Delta t}{\Delta x}(-2\beta c(\rho) - v_i^j)(v_{i+1}^j - v_i^j) - \frac{\Delta t}{\tau}(v_i^j - \overline{V}) + \frac{\Delta t}{\tau}\overline{V}'\left[\frac{(\rho_{i-1}^j - \rho_i^j)}{2\,\Delta x\,\rho_i^j}\right]; \tag{35}$$

b) For light traffic (i.e. $v_i^j \geq -2\beta\, c(\rho)$)

$$v_i^{j+1} = v_i^j + \frac{\Delta t}{\Delta x}(-2\beta\, c(\rho) - v_i^j)(v_i^j - v_{i-1}^j) - \frac{\Delta t}{\tau}(v_i^j - \overline{V}) + \frac{\Delta t}{\tau}\overline{V}'\left[\frac{(\rho_{i-1}^j - \rho_i^j)}{2\,\Delta x\,\rho_i^j}\right], \tag{36}$$

where index i represents the road section and index j represents time. Here Δt and Δx are the grid sizes of the finite difference mesh in time and space dimensions, respectively.

For the discretisation of the conservation equation (5), the difference format suitable for physical sense of traffic flow is applied.[19,21] For the motion equation (6) upwind scheme is used. The above difference scheme is suitable for the traffic flow as it maintain the physical properties of the traffic flow even under the extreme conditions. For example, let us consider that at any time 't_1', the density of any section x_1 is zero i.e. $\rho_{x_1}^{t_1} = 0$, then we have

$$\frac{\partial \rho_{x_1}^{t_1}}{\partial t} = \frac{1}{\Delta x}\left[\rho_{x_1-1}^{t_1} v_{x_1}^{t_1} - \rho_{x_1}^{t_1} v_{x_1+1}^{t_1}\right]. \tag{37}$$

Since $\rho_{x_1}^{t_1} = 0$ and $\rho_{x_1-1}^{t_1}\, v_{x_1}^{t_1} \geq 0$, we get

$$\frac{\partial \rho_{x_1}^{t_1}}{\partial t} \geq 0. \tag{38}$$

This implies that the density will never be negative after the time 't_1'. On the other hand, let us assume that at any time 't_1', the density of any section is maximum i.e. $\rho_{x_1}^{t_1} = \rho_m$ then we have

$$v_{x_1}^{t_1} = 0 \quad (\text{as } \rho_m \text{ is the jam density}). \tag{39}$$

Since $\rho_{x_1-1}^{t_1} v_{x_1}^{t_1} = 0$ and $\rho_{x_1}^{t_1} v_{x_1+1}^{t_1} \geq 0$, we get

$$\frac{\partial \rho_{x_1}^{t_1}}{\partial t} \leq 0, \tag{40}$$

which implies that density can not be greater than the maximum density. We can apply similar type of analyses for the speed also.

5.2. Numerical examples

In this section, we illustrate the results of previous section with some numerical examples. In order to test the traffic flow stability condition, macroscopic simulation is presented using a hypothetical ring road of 32.2 km long. Let us consider the behaviour of a localised perturbation, which at time $t = 0$, occurs in an initial homogeneous state of traffic flow and is given by

$$\rho(x,0) = \begin{cases} \rho_0 + a\rho_0 \cos\left(\dfrac{\pi\,(x - x_0)}{2l}\right), & x_0 - l \leq x \leq x_0 + l; \\ \rho_0, & \text{otherwise}, \end{cases} \tag{41}$$

$$v(x,0) = \overline{V}(\rho(x,0)), \quad x \in [0,L], \tag{42}$$

where $x_0 = 0.6L$ and L is the length of road section under consideration. Here, $a = 0.15$ is the perturbation coefficient and $l = 12\Delta x$ is the perturbation radius. The periodic boundary condition for simulation to describe the amplification of disturbances is used and is given by

$$\rho(L,t) = \rho(0,t), \quad v(L,t) = v(0,t). \tag{43}$$

For equilibrium speed–density relationship, we use the following relation proposed by Kerner and Konhäuser.[10]

$$\overline{V}(\rho) = u_{\mathrm{f}} \left[\left(1 + \exp\left(\frac{\frac{\rho}{\rho_{\mathrm{m}}} - 0.25}{0.06} \right) \right)^{-1} - 3.72 \times 10^{-6} \right], \tag{44}$$

where u_{f} is the free flow velocity and ρ_{m} is the jam density. For computational purpose, the space domain is divided into equal intervals of length 200 m and time interval is chosen as 1 s.

We take two different sets of parameter to show that our model can also describe nonlinear stability of traffic flow.[10,34,35]

$$\beta = 2.0, \quad u_{\mathrm{f}} = 30 \text{ m/s}, \ \tau = 10 \text{ s} \ \text{ and } \ \rho_{\mathrm{m}} = 0.2 \text{ veh/m}; \tag{45}$$

$$\beta = 5.0, \quad u_{\mathrm{f}} = 40 \text{ m/s}, \ \tau = 30 \text{ s} \ \text{ and } \ \rho_m = 0.2 \text{ veh/m}. \tag{46}$$

The critical values ρ_{c_1} and ρ_{c_2} corresponding to the parameters (45) and (46) are 0.041, 0.084 and 0.046, 0.076 respectively, which can easily be found out by substituting the parameter values into the stability condition (33). The traffic flow will be unstable between these critical densities. Taking different values of initial density for both the sets of parameter, we investigate the traffic density pattern with respect to time and results for two different values of β are shown in Figs. 1 and 2.

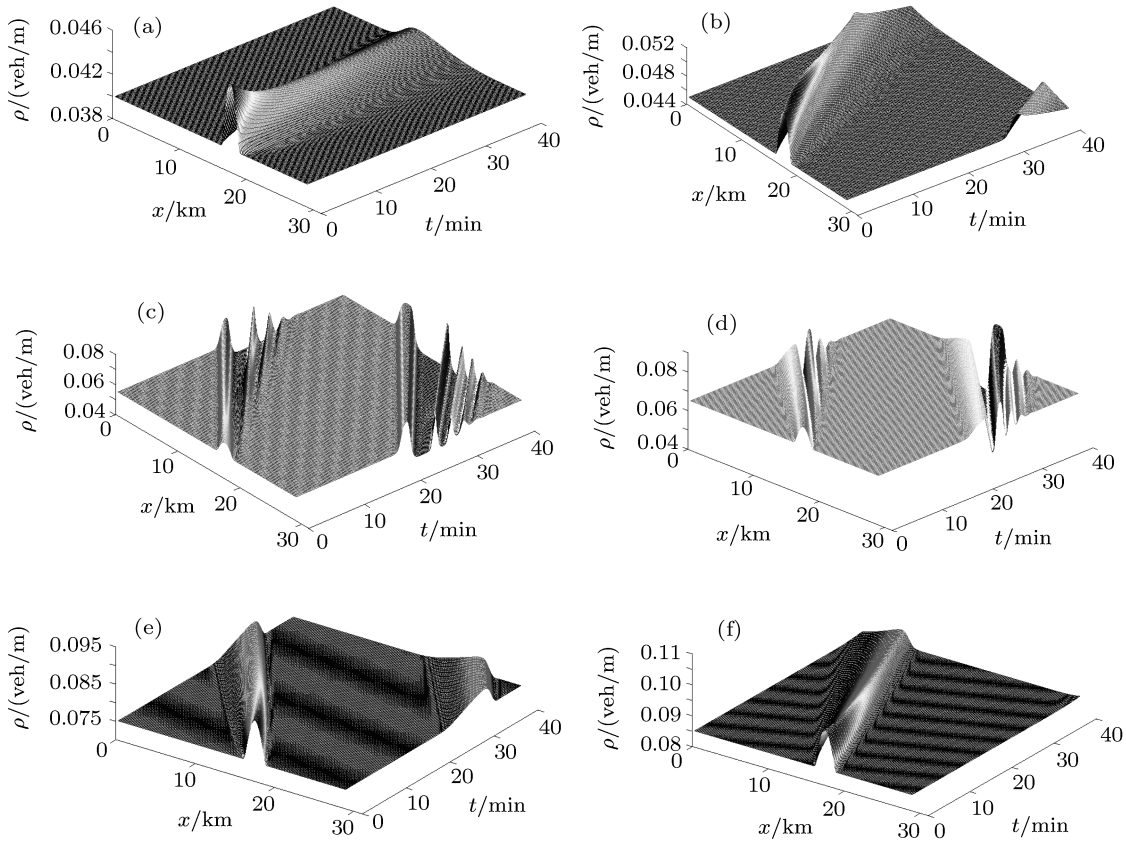

Fig. 1. Temporal evolution of traffic density on a ring road of circumference 32.2 km with a homogeneous initial condition (45) and a localised perturbation for (a) $\rho_0 = 0.04$ veh/m, (b) $\rho_0 = 0.045$ veh/m, (c) $\rho_0 = 0.055$ veh/m, (d) $\rho_0 = 0.065$ veh/m, (e) $\rho_0 = 0.075$ veh/m, (f) $\rho_0 = 0.085$ veh/m.

In Fig. 1(a), the traffic flow density is very low and the perturbation dies out with time, which shows a good agreement with the Herrmann and Kerner theory[35] that below the critical density, the initially homogeneous state of traffic flow is stable with respect to the growth of any non-homogeneous perturbations. As the initial density increases, the amplitude of the initial large perturbations grows in time. Figure 1(b) shows that when the initial density is just above the down critical density, the high density and low velocity region still exists, but it becomes triangle-like and width of this region are not constant. This situation corresponds to stop-and-go traffic. Further increase in initial density leads to a dipole-like structure as illustrated by Figs. 1(c) and 1(d) in which a complex localised structure of two or more clusters forms. In Fig. 1(d) the density of the cluster increases more rapidly than in Fig. 1(c). It is clear from Figs. 1(e) that the non-homogeneous perturbations are first decreases and after some time becomes stable and non-stationary when the initial density is nearer to the up critical density. Finally, when the density becomes greater than the up critical density, a stable regime is reached again slowly as can be seen in Fig. 1(f).

Similarly, Fig. 2 describes the growth of the localised perturbation for different values of initial density with the parameters given in Eq. (46). The results are found to be the same as the results for the parameter values in Eq. (45) and shown graphically by Figs. 2(a)–2(e). It is observed that for $\beta = 5$, the shape of the cluster for different initial data is the same. Figure 2 illustrates that with the growth of the large amplitude perturbations, a non-stationary cluster of triangular shape forms. Firstly, the perturbation decreases and as time increases the amplitude of the perturbation increases. The cluster of vehicles represents a locally moving region, where the density is higher and the average velocity is lower than the initial flow and outside the cluster.

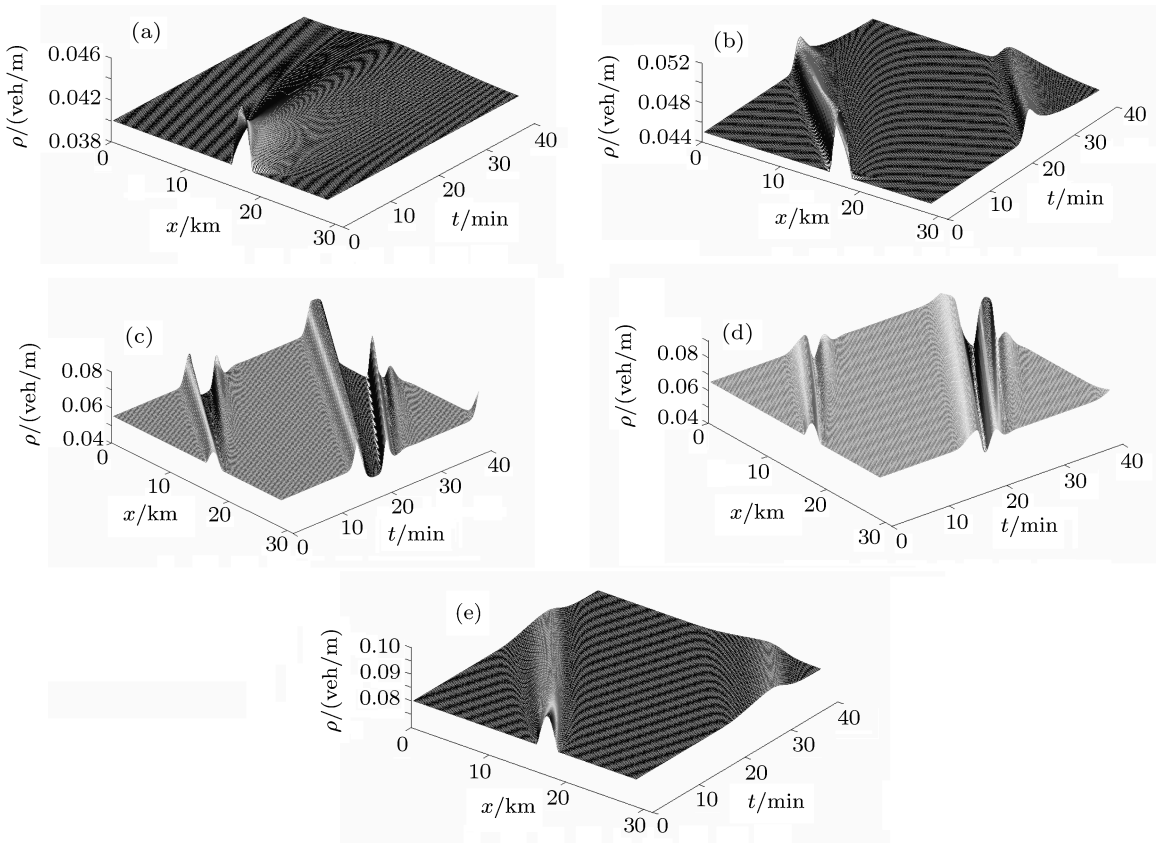

Fig. 2. Temporal evolution of traffic density on a ring road of circumference 32.2 km with a homogeneous initial condition (46) and a localised perturbation for (a) $\rho_0 = 0.04$ veh/m, (b) $\rho_0 = 0.048$ veh/m, (c) $\rho_0 = 0.055$ veh/m, (d) $\rho_0 = 0.065$ veh/m, (e) $\rho_0 = 0.08$ veh/m.

For both the values of anisotropic parameter, we observe that there are two perturbed waves generated by the initial conditions: one is moving forwards and the other is backwards. The magnitude of the forward wave is much smaller than that of the backward wave. Moreover the forward wave disappears quickly and the backward wave does not.

Therefore, the above result shows a good agreement with the results found by Yi *et al.*[27] and Ou *et al.*[28,29]

6. Conclusion

In the literature of macroscopic traffic-flow theory, the model plays an important role in explaining certain aspects of the system. The applicability of all the existing higher order macroscopic vehicular traffic flow models depends on their capability to reproduce nonlinear traffic flow behaviour observed in real traffic.

In this paper, we investigated an anisotropic continuum traffic flow model, recently proposed by Gupta and Katiyar.[19,20] Our model is anisotropic and also overcomes the problem of negative flows and negative speeds (i.e., wrong-way travel). A traffic flow model usually needs stability analysis and numerical simulation in the stable and unstable density regions in order to investigate the evolution of a traffic initial state. Since in the linear stability analysis higher-order terms are neglected, we propose a nonlinear stability analysis by utilising a wavefront expansion technique under large traffic disturbances. In comparison with the linear stability analysis, the nonlinear stability analysis additionally gives the analytical solution of the slope of the wavefront, and then the evolution of disturbances with time can be illuminated by stability parameters and initial conditions. We presented a simple finite difference scheme to carry out the numerical simulation and discuss the applicability of the scheme in some special cases. We investigated numerically the shock wave propagation and vehicle clustering in the anisotropic continuum model on a circular road. Comparing the numerical results with those presented by Yi *et al.*[27], Ou *et al.*,[28,29] we find that the clusters have almost the same structure for different values of the anisotropic parameter. The numerical results confirm the stability analysis for our model.

Further investigations need to be carried out to test the performance of the new anisotropic continuum model in modelling real traffic. So it may be reasonable to conclude that the stability condition found in this work can be further used for the prediction of traffic stability and to perform a qualitative analysis of the relationships between traffic behaviours and traffic model parameters and results obtained are consistent with the spectrum of nonlinear dynamic properties reported in the literature.

Acknowledgments

The authors are grateful to the anonymous referees for their suggestions to improve the paper.

References

[1] Gerlough D L and Huber M J 1975 *Special Report* No **165** (Washington, DC: Transportation Research Board, National Research Council)
[2] Helbing D 2001 *Rev. Mod. Phys.* **73** 1067
[3] Wong G C K and Wong S C 2002 *Trans. Res.* A **36** 827
[4] Lighthill M J and Whitham G B 1955 *Proc. R. Soc. London* Ser. A **229** 317
[5] Richards P I 1956 *Operations Research* **4** 42
[6] Zhang H M 2003 *Trans. Res.* B **37** 101
[7] Lax P D 1972 *Society for Industrial and Applied Mathematics* (Philadelphia, PA)
[8] Payne H J 1971 *Mathematical Models of Public Systems* In: Bekey G A (Ed.) *Simulation Councils Proceedings Series* **1** 51
[9] Phillips W F 1979 *Trans. Plann. Technol.* **5** 131
[10] Kerner B S and Konhäuser P 1993 *Phys. Rev.* E **48** 2335
[11] Zhang H M 1998 *Trans. Res.* B **32 (7)** 485
[12] Berg P, Mason A and Woods A 2000 *Phys. Rev.* E **61** 1056
[13] Bando M, Hasebe K, Nakayama A, Shibata A and Sugiyama Y 1995 *Phys. Rev.* E **51** 1035
[14] Daganzo C F 1995 *Trans. Res.* B **29** 277
[15] Zhang H M 2000 *Trans. Res.* B **34** 583
[16] Treiber M, Hennecke A and Helbing D 1999 *Phys. Rev.* E **59** 239
[17] Zhang H M 2002 *Trans. Res.* B **36** 275
[18] Zhang H M 2003 *Trans. Res.* B **37** 27
[19] Gupta A K and Katiyar V K 2005 *J. Phys.* A **38** 4069
[20] Gupta A K and Katiyar V K 2006 *Physica* A **368** 551
[21] Jiang R, Wu Q and Zhu Z 2002 *Trans. Res.* B **36** 405
[22] Holland E N 1998 *Trans. Res.* B **32** 141
[23] Whitham G B 1974 *Linear and Nonlinear Waves* (New York: John Wiley & Sons Inc)
[24] Swaroop D and Rajagopal K R 1999 *Trans. Res.* C **7** 329
[25] Zhang H M 1999 *Trans. Res.* B **33** 399
[26] Del Castillo J M 2001 *Trans. Res.* B **35** 367
[27] Yi J G, Lin H, Alvarez L and Horowitz R 2003 *Trans. Res.* B **37** 661
[28] Ou Z H, Dai S Q, Zhang P and Dong L Y 2007 *SIAM J. Appl. Math.* **67** 605
[29] Ou Z H 2005 *Physica* A **351** 620
[30] Ou Z H, Dai S Q, Dong L Y, Wu Z and Tao M D 2006 *Physica* A **362** 525
[31] Helbing D and Johansson A F 2009 *Eur. Phys. J.* B **69** 549
[32] Zhang H M 2009 *Eur. Phys. J.* B **69** 563
[33] Helbing D 2002 *Math. Comput. Modelling* **35** 517
[34] Kerner B S and Konhäuser P 1994 *Phys. Rev.* E **50 (1)** 54
[35] Herrmann M and Kerner B S 1998 *Physica* A **255** 163